Journal of Power Sources 190 (2009) 417–422

Contents lists available at ScienceDirect

Journal of Power Sources

journal homepage: www.elsevier.com/locate/jpowsour

Electrophoretic deposition of dense $BaCe_{0.9}Y_{0.1}O_{3-x}$ electrolyte thick-films on Ni-based anodes for intermediate temperature solid oxide fuel cells

Milan Zunic[a,b,*], Laure Chevallier[a], Francesca Deganello[c], Alessandra D'Epifanio[a], Silvia Licoccia[a], Elisabetta Di Bartolomeo[a], Enrico Traversa[a]

[a] Dipartimento di Scienze e Tecnologie Chimiche, Università di Roma "Tor Vergata", Via della Ricerca Scientifica, 00133 Rome, Italy
[b] Institute for Multidisciplinary Research, Kneza Viseslava 1a, 11000 Belgrade, Serbia
[c] CNR-ISMN, Via Ugo La Malfa, 153, 90146 Palermo, Italy

ARTICLE INFO

Article history:
Received 18 September 2008
Received in revised form 20 December 2008
Accepted 18 January 2009
Available online 15 February 2009

Keywords:
Fuel cells
Thick film
Electrophoretic deposition
Cermet
Protonic conductor

ABSTRACT

Proton conducting $BaCe_{0.9}Y_{0.1}O_{3-x}$ (BCY10) thick films are deposited on cermet anodes made of nickel–yttrium doped barium cerate using electrophoretic deposition (EPD) technique. BCY10 powders are prepared by the citrate–nitrate auto-combustion method and the cermet anodes are prepared by the evaporation and decomposition solution and suspension method. The EPD parameters are optimized and the deposition time is varied between 1 and 5 min to obtain films with different thicknesses. The anode substrates and electrolyte films are co-sintered at 1550 °C for 2 h to obtain a dense electrolyte film keeping a suitable porosity in the anode, with a single heating treatment. The samples are characterized by field emission scanning electron microscopy (FE-SEM) and energy dispersion spectroscopy (EDS). A prototype fuel cell is prepared depositing a composite $La_{0.8}Sr_{0.2}Co_{0.8}Fe_{0.2}O_3$ (LSCF)–$BaCe_{0.9}Yb_{0.1}O_{3-\delta}$ (10YbBC) cathode on the co-sintered half cell. Fuel cell tests that are performed at 650 °C on the prototype single cells show a maximum power density of 174 mW cm^{-2}.

1. Introduction

The reduction of the operating temperature of solid oxide fuel cells (SOFCs) below 700 °C (intermediate temperature, IT) allows the use of low cost and durable sealant and interconnects, yields faster start-up times for portable use, increases stability, and diminishes excessive power consumption requested by high temperature SOFC operation [1–4]. However, the electrolyte conductivity and the efficiency of fuel cells are significantly reduced. One possible solution to this issue is to decrease the electrolyte thickness, thereby resulting in its internal resistance reduction [5,6].

Recently, many considerable efforts have been made to produce thin and thick electrolyte films. Various deposition techniques have been exploited such as physical vapor deposition (PVD) [7,8], chemical vapor deposition (CVD), combustion chemical vapor deposition (CCVD) [9], electrochemical vapor deposition (ECVD) [10,11] or plasma technologies [12]. Dense films of yttria-stabilized zirconia (YSZ) electrolyte were successfully deposited on calcia-stabilized zirconia porous [10] or non-porous [12] tube, and on NiO-doped ceria pellet [11], but all these techniques have the drawbacks of requiring extreme experimental conditions, such as high temperature and very low pressure, together with sophisticated and costly equipment. Moreover, these techniques can only be used with a restricted number of ceramic materials and restricted substrate shape.

Electrophoretic deposition (EPD) has been recognized as a simple, rapid and reproducible coating technique that has a huge potential for economic manufacture of dense, gas tight, and thick films [13]. However, EPD is still not a widespread method for deposition of dense electrolyte films for SOFCs, even though it has been already used for deposition of oxygen ion conductor electrolytes on anode or cathode porous substrates [14–19].

Two main issues have to be solved for successful EPD of dense, uniform, and crack-free thick-films: the choice of the suspension medium, which can stabilize the dispersion of electrically charged particles, and the optimization of the conductivity properties of the substrate. Different organic solvents have been tested as suspending media, like benzene, ketones or iodine added acetone [13,20,21]. Metallic substrates [15] or thin graphite layers decomposed during sintering [16] have been used as conductive substrates for deposition, despite they are not properly suitable for SOFC applications. Typical green or pre-sintered NiO–YSZ substrates for anode-supported SOFCs are not conductive at room temperature. Nevertheless, optimizing their microstructure and porosity [13] or

* Corresponding author at: Department of Chemical Science and Technology, University of Rome Tor Vergata, Via della Ricerca Scientifica, 1, 00133 Rome, Italy. Tel.: +39 06 7259 4495; fax: +39 06 7259 4328.
E-mail address: milan.zunic@uniroma2.it (M. Zunic).

0378-7753/$ – see front matter © 2009 Elsevier B.V. All rights reserved.
doi:10.1016/j.jpowsour.2009.01.046

adding graphite both as porogen and electronic conductor [19,22], it is possible to achieve a green anode conductivity value adequate for EPD deposition.

In this work, EPD was developed to obtain dense films of $BaCe_{0.9}Y_{0.1}O_{3-x}$ (BCY10) protonic conductor on optimized green nickel–yttrium doped barium cerate (NiO–BCY10) anode. EPD suspension was made up of BCY10 powder and iodine-dissolved acetylacetone solvent without any binder or dispersing agent. The anodes were prepared by a liquid mixture technique mixing binder, NiO–BCY10 cermet powder and graphite in water [23]. Cathodic electrophoretic deposition process was performed at constant voltage varying the deposition time and thus obtaining films with different thicknesses. The substrates with deposited BCY10 films were slowly dried, to avoid the formation of cracks, then pre-fired at 1000 °C, and finally sintered at 1550 °C. The optimized co-sintering process of substrate and deposited film ensured to get homogeneous, dense thick films coupled to anodes with suitable porosity. Single cells were prepared by adding a composite cathode material [24] and cell tests were performed for the first time, to the best of our knowledge, on single protonic fuel cells prepared by EPD method.

2. Experimental

2.1. Preparation of BCY10 powder

The protonic conductor material was prepared by citrate–nitrate auto-combustion method using $Ba(NO_3)_2$ (Aldrich, 99.999%), $Ce(NO_3)_2{\cdot}6H_2O$ (Aldrich, 99.999%) and $Y(NO_3)_2{\cdot}6H_2O$ (Aldrich, 99.9%) as starting reactants and citric acid as combustion fuel. This synthesis has been described in details elsewhere [25]. The obtained powder was fired at 1000 °C for 10 h and characterized by X-ray diffraction (XRD, Philips X'pert D500) analysis and field emission scanning electron microscopy (FE-SEM, Leo Supra 1250).

2.2. Substrate preparation

To get uniform distribution of NiO grains in BCY10 ceramic, NiO–BCY10 composite powders were prepared by using a wet-chemical route [23]. The starting reactants were $Ni(NO_3)_2{\cdot}6H_2O$ (Aldrich, 99.99%) and BCY10. The weight ratio between Ni and BCY10 was set to 1:1. The resulting powders were milled in an agate mortar and calcined at 1000 °C for 5 h.

The anode slurry was prepared mixing PVA (polyvinyl alcohol, Aldrich, 99.9%), NiO–BCY10 cermet powder and graphite powder (<20 μm, Aldrich) in water. Anode preparation has been described in details elsewhere [23]. The weight ratio between NiO–BCY10, graphite, and PVA was 70:25:5, respectively. Cylindrical pellets with a diameter of 13 mm and a thickness of about 0.7 mm were uniaxially pressed at 150 MPa and used as electrically conductive anode substrates.

2.3. Suspension preparation

EPD suspension was made up of BCY10 powder and iodine-dissolved acetylacetone solvent (Aldrich). The concentration of BCY10 powder and iodine in acetylacetone was optimized by trial and error approach and fixed to 8 and 0.37 g L^{-1}, respectively. Among several investigated solvents, iodine-dissolved acetylacetone was found to be the best in terms of suspension stability and deposition features.

Iodine was used to positively charge the BCY10 particles since protons were formed according to the following reaction [15]:

$$CH_3COCH_2COCH_3 + 2I_2 \leftrightarrow ICH_2COCH_2COCH_2I + 2I^- + 2H^+ \quad (1)$$

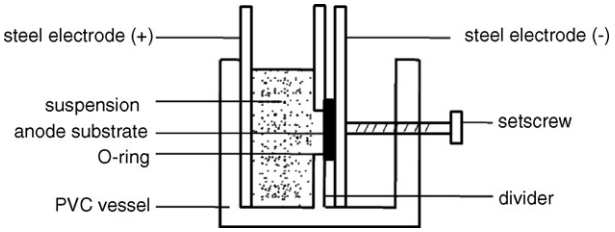

Fig. 1. Scheme of the EPD cell.

This reaction of iodine affects the suspension properties, such as its conductivity [26]. Thus, several suspensions were treated for 1 h in an ultrasonic bath and then steadied for different times ranging from 1 to 96 h. The sediments were always removed from the suspension to keep only the smaller BCY10 particles suspended for the EPD process. The best deposition in terms of homogeneity was obtained by using the suspension steadied for 72 h. Differently from many EPD processes where the addition of suitable additives are required [17,27], no binders or dispersing agents were used in our investigation to avoid possible contamination of the electrolyte.

2.4. Deposition procedure

Cathodic electrophoretic deposition process was performed at a constant voltage varying the deposition time, by using a high voltage dc power supply unit (BIO RAD, PowerPack 1000).

Fig. 1 shows a schematic view of the home-made EPD set-up. The anode substrate of NiO–BCY10 was fixed by a setscrew and connected to the negative output of the power source using a steel electrode. A second steel electrode, mounted in parallel to the other, was connected to the positive output. The distance between the positive electrode and the anode substrate was fixed to 15 mm. The anode substrate was exposed to the EPD suspension through a circular window arranged on the PVC divider. The anode substrate and the PVC divider were mechanically sealed to prevent any leakage of the suspension into the dry part of the vessel.

As the constant voltage was applied, positively charged particles of BCY10 were deposited on the anode substrate. The substrates with deposited BCY10 films were slowly dried at room temperature [28], to avoid the formation of cracks. After drying, samples were pre-fired at 1000 °C to burn all graphite powder and then sintered at 1550 °C for 2 h, using a heating ramp of 3 °C min^{-1}. During sintering, the deposited BCY10 films were covered with a BCY10 pellet to protect the EPD deposited films from barium evaporation at temperatures above 1200 °C. After sintering, the diameter of deposited electrolyte was 7.95 mm and the thickness of anode was 0.45 mm.

XRD analysis, FE-SEM observations, and energy dispersion X-ray (EDAX, INCA Energy 300) analysis were used to analyze the crystal structure, morphology, and chemical composition of the sintered films and anodes.

2.5. Fuel cells preparation and testing

Hydrogen–air fuel cell experiments were carried out at 600 and 650 °C. The single cells were prepared by brush painting the cathode powders mixed with a commercial screen-printing oil on BCY10 dense film and then firing at 1100 °C for 2 h. Composite cathode powders, $La_{0.8}Sr_{0.2}Co_{0.8}Fe_{0.2}O_3$ (LSCF)–$BaCe_{0.9}Yb_{0.1}O_{3-\delta}$ (10YbBC), were used, specifically optimized for BCY proton conductor electrolyte [24]. The diameter of cathode active area was 6 mm ($A = 0.283\ cm^2$), which is smaller than the electrolyte diameter (7.95 mm). We choose a smaller diameter to avoid a short circuit contact between cathode and anode during the cathode painting procedure. The thickness of the cathode was 80 ± 5 μm.

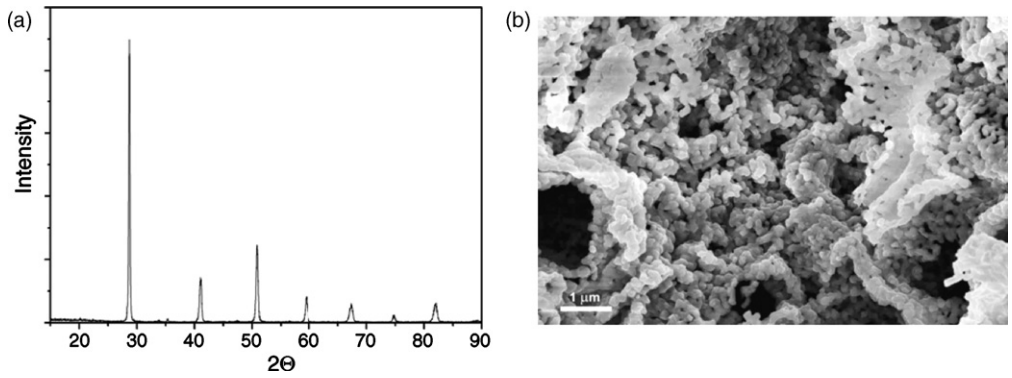

Fig. 2. XRD pattern (a) and SEM micrograph (b) of the BCY10 powder calcined at 1000 °C for 10 h.

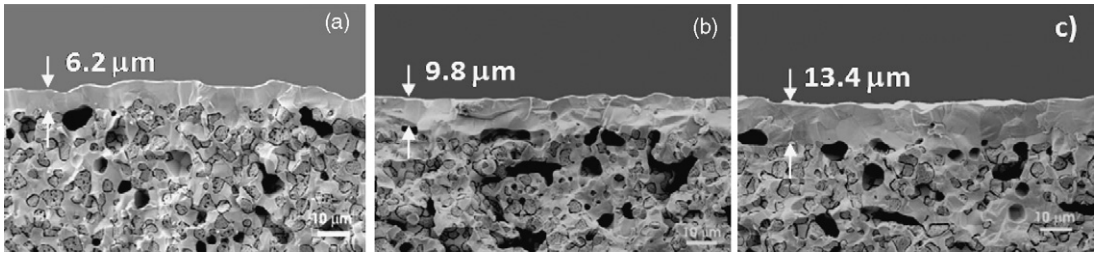

Fig. 3. SEM micrographs of the cross-sections of: EPD 1 (a), EPD 2 (b) and EPD 3 (c) BCY10 films on NiO–BCY10 anode substrate, co-sintered at 1550 °C for 2 h.

Gold wires were fixed with a drop of platinum paste (Engelhard-Clal) on the top of the anode and cathode and used as current collectors. For the fuel cell tests, the samples were mounted at the end of an alumina tube using a gas tight ceramic paste seal (Aremco, 552). The anode was exposed to wet hydrogen (3 vol.% H_2O) while the cathode was exposed to ambient air. The electrochemical measurements were performed using a multichannel potentiostat VMP3 (Princeton Applied Research). The impedance was measured in the frequency range of 500 kHz–0.1 Hz with the signal amplitude of 10 mV under open-circuit condition. The cell was equilibrated at open-circuit for about 10 min before the electrochemical impedance spectroscopy (EIS) measurement.

3. Results and discussion

Fig. 2(a and b) shows the XRD pattern and FE-SEM images of the BCY10 powders, respectively. The citrate–nitrate auto-combustion method allowed us to obtain BCY10 powders with a single orthorhombic phase (JCPDS 81-1386) and a sponge-like microstructure with an average grain size of less than 100 nm.

By using the suspension based on the BCY10 nanopowders, electrophoretic deposition was carried out at a constant voltage of 40 V with a deposition time varying from 1 to 5 min (Table 1) on NiO–BCY10 anode substrates. The working conditions and the current values measured during the deposition are reported in Table 1, together with the labeling of the samples prepared.

Fig. 3(a–c) shows the SEM micrographs (cross sections) of the co-sintered EPD 1, EPD 2, and EPD 3 films on the anode substrate. The BCY10 deposited films were dense and the anode–electrolyte interface showed a good interfacial adhesion. Regarding the anode substrates, it was checked that the NiO particles were well dispersed in the BCY10 matrix and that a continuous network of BCY10 was formed. The anode macroporosity required for gas permeation was also clearly noticeable.

Table 1
Parameters of constant voltage electrophoretic deposition.

Name	Voltage (V)	Time (min)	Measured current (mA)
EPD 1	40	1	3.1 → 1.1
EPD 2	40	3	3.1 → 0.6
EPD 3	40	5	3.1 → 0.4

By increasing the deposition time from 1 to 5 min, a film thickness growth from 6.2 to 13.4 µm was observed, as reported in Fig. 3. The thickness of deposited films was measured at different locations along the cross-section of individual samples. The average values were plotted versus time and a linear trend was noticed, as shown in Fig. 4. These results are in agreement with some literature data on EPD of other materials [29].

Fig. 5(a and b) shows the SEM micrographs (top view) of EPD 1 and EPD 3 samples. Sintered nanometric grains were obtained for both BCY10 films. The EPD deposition time did not significantly affect the shape and dimension of the BCY10 grains. The only slight

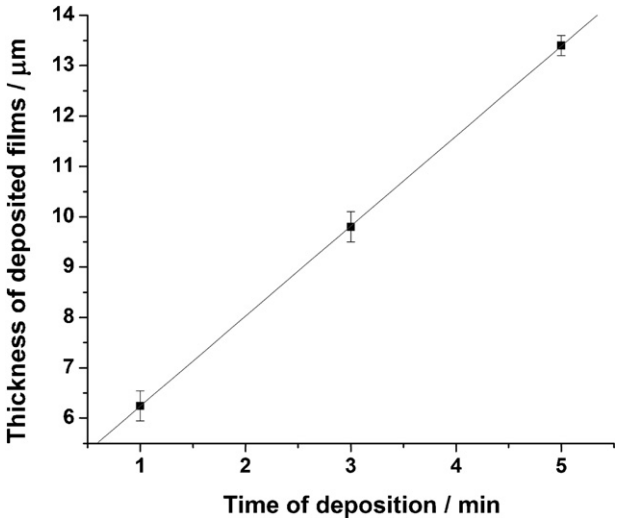

Fig. 4. Influence of the deposition time on the deposited film thickness. For each sample average values are reported, together with minimum and maximum values.

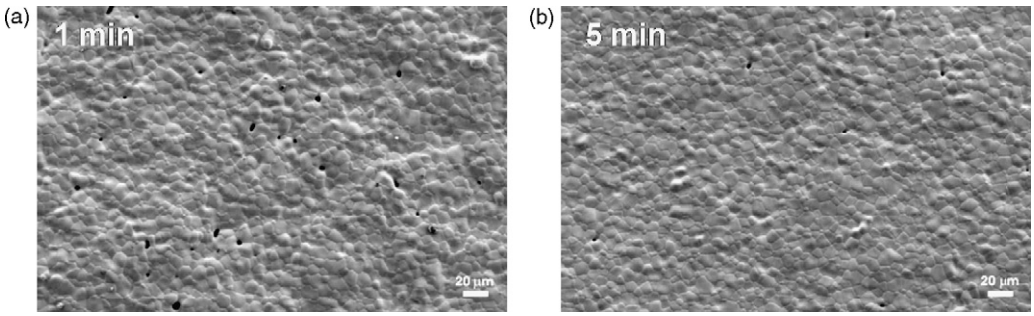

Fig. 5. SEM micrographs (top view) of EDP 1 (a) and EDP 3 (b) films co-sintered at 1550 °C for 2 h.

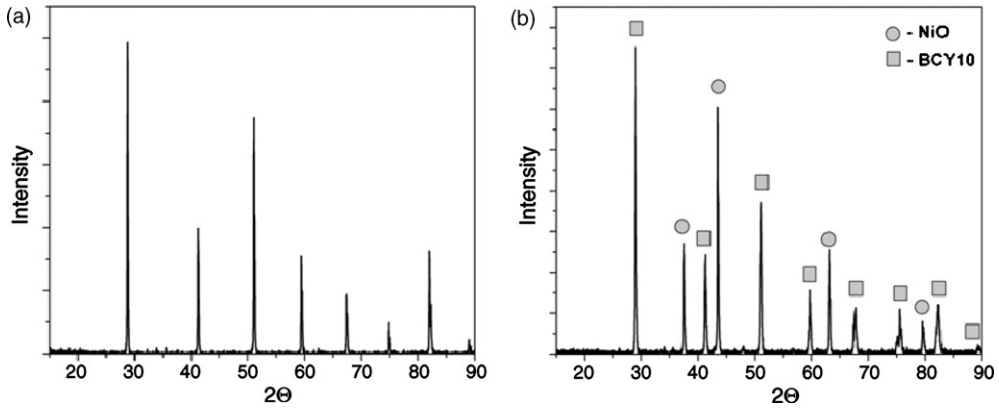

Fig. 6. XRD patterns of EPD 3 film (a) and NiO–BCY10 anode substrate (b) after sintering at 1550 °C.

difference in morphology was the porosity. Comparing Fig. 5(a) and (b), it was seen that with the shorter deposition time the larger porosity with bigger pinholes and micropores was obtained. If the deposition time was too short (1 min), an incomplete and thus not uniform deposition was obtained, leading to the formation of pores during the sintering process. On the other side, for a longer deposition time (5 min) a thicker and thus smoother and denser deposit could be obtained.

Fig. 6(a) shows the XRD pattern of EPD 3 film of BCY10 while Fig. 6(b) shows the XRD pattern of the NiO–BCY10 anode substrate, both after the sintering process. It was confirmed that the dense BCY10 electrolyte film was pure showing its typical orthorhombic phase. Thus, the evaporation or degradation of BCY10 film during the sintering process was successfully avoided. Regarding the anode substrate, the NiO (JCPDS 74-1299) and BCY10 (JCPDS 81-1386) phases could be observed without any secondary phase.

All these findings clearly show that the optimized co-sintering process of the EPD electrolyte film deposited on the green anodic substrate ensured to get homogeneous, fully dense BCY10 thick films preserving a suitable porosity within the anode substrates, despite the high sintering temperature.

According to these results, the NiO–BCY10/EPD 3/LSCF–10YbBC cell, with a 13.4 μm BCY10 electrolyte thick film, was chosen for preliminary fuel cell tests. Fig. 7 shows the SEM cross section micrograph of the single cell after measurements. The three material components of the fuel cell are clearly identified in the image. Both cathode–electrolyte and the anode–electrolyte interfaces showed good interfacial adhesion. The EPD deposited BCY10 thick film was fully dense, while the cathode showed a porous microstructure and submicrometric grain size. The anode confirmed its macro-

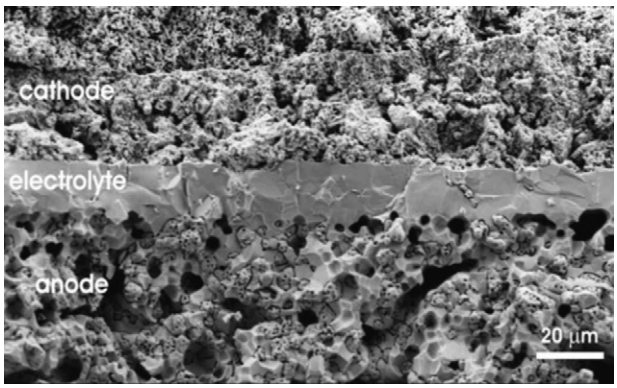

Fig. 7. SEM micrograph (cross-section view) of Ni–BCY10/BCY10/LSCF–10YbBC fuel cell, after electrochemical measurements.

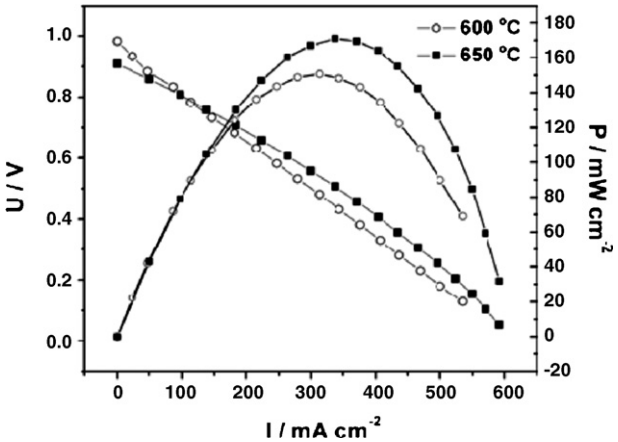

Fig. 8. *I–V* curves and power density output of Ni–BCY10/BCY10/LSCF–10YbBC cell measured at 600 and 650 °C in hydrogen–air fuel cell experiments.

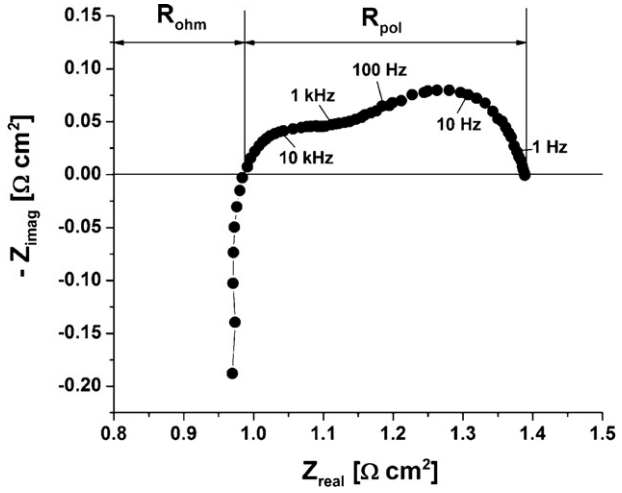

Fig. 9. Typical complex impedance plane plot of the Ni–BCY10/BCY10/LSCF–10YbBC fuel cell measured at 650 °C in wet H_2 (3 vol.% H_2O).

porosity necessary for fuel diffusion and continuous connections between Ni and BCY10 grains that assure uninterrupted pathways for electronic (Ni) and ionic (BCY10) conduction in the anode pellet.

Fig. 8 shows the *I–V* and power density output curves that were obtained by exposing the anode to wet H_2 and the cathode to ambient air at 600 and 650 °C. The measured open-circuit voltages (OCV) were 0.98 and 0.91 V at 600 and 650 °C, respectively, which were 89% and 85% of the theoretical values at 600 and 650 °C, respectively. This fact could be attributed to the existing small pinholes that do not fully prevent gas leakage through the BCY10 film, as shown in Fig. 5(b). Nevertheless, the OCV decreased more with increasing the operating temperature. At temperatures above 650 °C, it is well known that ambipolar conductivity can be present in BCY materials [30–32], which might also affect the decrease in OCV measured at 650 °C. However, a very promising performance was obtained both at 600 and 650 °C, since the maximum power densities were 150 and 174 mW cm^{-2}, respectively.

Electrochemical impedance spectroscopy (EIS) measurements were carried out in fuel cell measurement conditions at OCV, at 600 and 650 °C. Fig. 9 shows a typical complex impedance plot of the Ni–BCY10/BCY10/LSCF–10YbBC fuel cell in wet H_2 (3 vol.% H_2O), measured at 650 °C. The cell impedance at OCV is typically characterized by a larger arc at low frequencies and smaller arc at intermediate frequencies. This indicates that at least two different electrode processes corresponding to the high- and intermediate- frequency arcs exist. The typical electrode polarization resistance (R_{pol}) and ohmic resistance (R_{ohm}) of the cell are defined as the difference between the low and high frequency real axis intercepts in the complex impedance plane plot, and the high frequency real axis intercept, respectively [33]. The impedance pattern shows that the total cell resistance (R_{tot}) at 650 °C is determined primarily by ohmic resistance. The R_{ohm} value at 650 °C is 0.99 Ω cm^2 and R_{pol} is 0.39 Ω cm^2. While the relatively low value of R_{pol} shows good electrodes performances, the high value of R_{ohm} shows the existence of undesired ohmic losses in the cell. Based on the BCY10 protonic conductivity of ~0.01 S cm^{-1} at 650 °C [34], the ohmic resistance of the 13.4 μm thick film is estimated to be ~0.13 Ω cm^2. The large difference in ohmic resistance (~0.86 Ω cm^2) is probably due to the additional contact resistance at the LSCF–YbBC/BCY interface and the Ni–BCY/BCY interface as well as that at the electrodes and current collector interface.

4. Conclusions

BCY10 films having thickness smaller than 15 μm were successfully deposited on a green NiO–BCY10 composite anode by electrophoretic deposition. The starting suspension was composed of BCY10 nanopowders and iodine-dissolved acetylacetone. A co-sintering of the electrolyte and anode substrate at 1550 °C allowed us to obtain dense electrolyte films preserving a suitable porosity within the cermet anode, despite the severe sintering temperature. Preliminary hydrogen–air fuel cell tests using a composite cathode based on commercial LSCF and $BaCe_{0.9}Yb_{0.1}O_{3-\delta}$ showed a promising performance: a maximum power density of 174 mW cm^{-2} was measured at 650 °C. These preliminary results show that there is plenty of space to enhance the power density, and further work is now in progress to improve the anode and cathode composition and microstructure, and optimize the EPD parameters to obtain further thinner and denser electrolyte films. Also, further optimization of compatibility between electrodes and electrolytes should be done with an aim to decrease the interface contact resistance, which could result in the improvement of the fuel cell power density.

Acknowledgements

This work has been funded by the Ministry of University and Research (MiUR) of Italy under the frame of the FISR project "Polymeric and ceramic fuel cells: System validation and development of new materials" and of the PRIN project "Protonic Conducting Ceramics for Fuel Cells". We gratefully thank Emiliana Fabbri for the preparation of the composite cathode.

References

[1] O. Yamamoto, Electrochim. Acta 45 (2000) 2423–2435.
[2] A. Boudghene Stambouli, E. Traversa, Renewable Sustainable Energy Rev. 6 (5) (2002) 433–455.
[3] T. Norby, Solid State Ionics 125 (1999) 1–11.
[4] T. Hibino, A. Hashimoto, M. Suzuki, M. Sano, J. Electrochem. Soc. 149 (2002) A1503.
[5] J. Will, A. Mitterdorfer, C. Kleinlogel, D. Perednis, L.J. Gauckler, Solid State Ionics 131 (2000) 79–96.
[6] Y.J. Leng, S.H. Chan, K.A. Khor, S.P. Jiang, Intl. J. Hydrogen Energy 29 (2004) 1029–1033.
[7] X. Chen, N. Wu, A. Ignatiev, US patent no. 6,645,656 B1, 2003.
[8] B. Meng, X. He, Y. Sun, M. Li, Mater. Sci. Eng. B 150 (2008) 83–88.
[9] Z. Xu, J. Sankar, S. Yarmolenko, Surf. Coat. Technol. 177–178 (2004) 52–59.
[10] U.B. Pal, S.C. Singhal, J. Electrochem. Soc. 137 (1990) 2937–2941.
[11] A. Mineshige, K. Fukushima, K. Tsukada, M. Kobune, T. Yazawa, K. Kikuchi, M. Inaba, Z. Ogumi, Solid State Ionics 175 (2004) 483–485.
[12] Z. Ogumi, Y. Uchimoto, Y. Tsuji, Z. Takehara, J. Appl. Phys. 72 (1992) 1577–1582.
[13] L. Besra, M. Liu, Prog. Mater. Sci. 52 (2007) 1–61, and references therein.
[14] T. Ishihara, K. Sato, Y. Mizuhara, Y. Takita, Chem. Lett. (1992) 943–946.
[15] T. Ishihara, K. Sato, Y. Takita, J. Am. Ceram. Soc. 79 (4) (1996) 913–919.
[16] R.N. Basu, C.A. Randall, M.J. Mayo, J. Am. Ceram. Soc. 84 (1) (2001) 33–40.
[17] I. Zhitomirsky, A. Petric, J. Mater. Sci. 39 (2004) 825–831.
[18] J. Will, M.K.M. Hruschka, L. Gubler, L.J. Gauckler, J. Am. Ceram. Soc. 84 (2) (2002) 328–332.
[19] G. Savo, A. Rainer, A. D'Epifanio, S. Licoccia, E. Traversa, in: S.C. Singhal, J. Mizusaki (Eds.), Solid Oxide Fuel Cells IX (SOFC IX), vol. 2005–2007, The Electrochemical Society, Pennington, NJ, 2005, pp. 1031–1036.
[20] S. Okamura, T. Tsukamoto, N. Koura, Jpn. J. Appl. Phys. 32 (1993) 4182–4185.
[21] F. Bozza, R. Polini, E. Traversa, Fuel Cells 5 (2008) 344–350.
[22] K. Yamaji, H. Kishimoto, Y. Xiong, T. Horita, N. Sakai, H. Yokokawa, Solid State Ionics 175 (2004) 165–169.
[23] L. Chevallier, M. Zunic, V. Esposito, E. Di Bartolomeo, E. Traversa, Solid State Ionics (submitted for publication).
[24] E. Fabbri, S. Licoccia, E. Traversa, E. D. Wachsman, Fuel Cells, in press.
[25] F. Giannici, A. Longo, F. Deganello, A. Balerna, A.S. Aricò, A. Martorana, Solid State Ionics 178 (2007) 587–591.
[26] N. Koura, T. Tsukamoto, H. Shoji, T. Hotta, Jpn. J. Appl. Phys. 34 (1995) 1643–1647.
[27] I. Zhitomirsky, A. Petric, J. Eur. Ceram. Soc. 20 (2002) 2055–2061.
[28] P. Sarkar, Proceedings of the electrochemical society on electrophoretic deposition: fundamentals and applications, vol. 2002–2021, Pennington, USA, 2002, pp. 71–77.

[29] M. Matsuda, T. Hosomi, K. Murata, T. Fukui, M. Miyake, J. Power Sources 165 (2007) 102–107.
[30] K.D. Kreuer, Solid State Ionics 125 (1999) 285–302.
[31] W.G. Coors, Solid State Ionics 178 (2007) 481–485.
[32] E. Fabbri, A. D'Epifanio, E. Di Bartolomeo, S. Licoccia, E. Traversa, Solid State Ionics 179 (2008) 558–564.
[33] V. Esposito, E. Traversa, E.D. Wachsman, J. Electrochem. Soc. 152 (12) (2005) A2300.
[34] H. Iwahara, H. Uchida, K. Ono, K. Ogaki, J. Electrochem. Soc. 135 (2) (1988) 529–533.